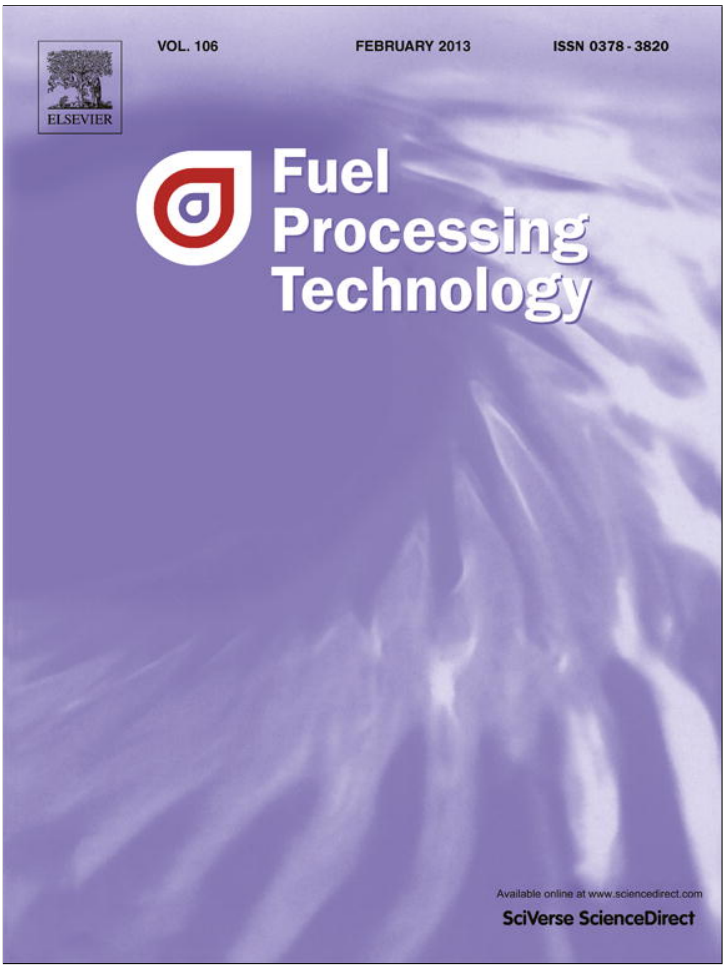

Fuel Processing Technology 106 (2013) 344–349

Contents lists available at SciVerse ScienceDirect

Fuel Processing Technology

journal homepage: www.elsevier.com/locate/fuproc

Synthesis of C_2 oxygenates from syngas over monodispersed SiO_2 supported Rh-based catalysts: Effect of calcination temperature of SiO_2

Jun Yu, Dongsen Mao *, Lupeng Han, Qiangsheng Guo, Guanzhong Lu

Research Institute of Applied Catalysis, School of Chemical and Environmental Engineering, Shanghai Institute of Technology, Shanghai 201418, PR China

ARTICLE INFO

Article history:
Received 8 May 2012
Received in revised form 19 August 2012
Accepted 24 August 2012
Available online 11 September 2012

Keywords:
Monodispersed SiO_2
Rh-based catalyst
CO hydrogenation
C_2 oxygenates
Calcination temperature

ABSTRACT

The effect of calcination temperature of the monodispersed SiO_2 synthesized by the Stöber method on the catalytic performance of Rh–Mn–Li/SiO_2 for CO hydrogenation to C_2 oxygenates was investigated. The means of N_2 adsorption-desorption, *in-situ* FT-IR, H_2-TPD, H_2-TPR, CO-TPD, and TPSR were used to characterize the physico-chemical properties of SiO_2 supports and the corresponding Rh–Mn–Li/SiO_2 catalysts. The results showed that the amount of surface Si-OH groups on SiO_2 affects the Rh dispersion and Rh–Mn interaction. The increase in the number of Si–OH groups on the SiO_2 was favorable for the Rh dispersion and CO adsorption, further enhanced the activity of the catalyst. In addition, an appropriate amount of surface Si–OH groups on the SiO_2 calcined at 350 °C can gain a moderate Rh–Mn interaction. This interaction is conducive to achieve the right hydrogenation ability, which is favorable for the CO insertion into metal-CH_x band, and ultimately increases the selectivity of C_2 oxygenates.

1. Introduction

The finite crude oil resources along with environmental concerns have stimulated a broad intensive search for processes to provide alternative feedstock for chemicals and fuels [1]. The synthesis of C_2 oxygenates (e.g., ethanol, acetaldehyde and acetic acid) from synthesis gas (syngas), which can be produced from non-petroleum carbon resources including natural gas, coal, and biomass, constitutes an alternative pathway for the production of clean fuels and chemicals [2–5]. However, the catalytic conversion of syngas to C_2 oxygenates remains challenging, and no commercial process exists as of today although extensive efforts have been made.

So far, Rh-based catalyst exhibits the most practical application due to its good performance for C_2 oxygenates synthesis [6–9]. The effect of the support on the selectivity towards C_2 oxygenates has been thoroughly investigated [10]. SiO_2 is one of the most extensively used supports for Rh-based catalysts, and its surface properties play an important role in determining the catalytic properties [11–14]. In our previous studies, it was found that the catalytic performance of the Rh–Mn–Li/SiO_2 catalyst for the synthesis of C_2 oxygenates from CO hydrogenation was enhanced greatly when a commercial SiO_2 was replaced by a monodispersed SiO_2 prepared by the Stöber method [15]. It was also proved that the hydroxyl-metal interaction over the Rh–Mn–Li catalyst supported on different silica resulted in a change in the CO adsorption on Rh particles, leading to significantly different catalytic activities [15]. In fact, it is widely accepted that the promoter/Rh boundary plays a key role in generating the required active sites for the selective synthesis of C_2 oxygenates [16–18], while the hydroxyl concentration may affect the interaction between neighboring cations or atoms on the support [16].

Considering that the concentration of surface hydroxyls on silica may influence greatly the properties of the supported metal component, the effect of calcination temperature of the monodispersed SiO_2 on the performance of Rh–Mn–Li/SiO_2 catalysts was further investigated in this work. With regard to the additives, it has been reported that Mn and Li can improve the CO conversion and oxygenates selectivity, respectively [8]. In order to compare the catalytic performance of the catalysts more clearly, here we took a known recipe of Rh–Mn–Li [15], as a part of screening for catalysts with a high activity and C_2 oxygenates selectivity. Then, CO hydrogenation performance of the catalysts was correlated with the interaction extents among Rh, Mn and SiO_2.

2. Experimental

2.1. Catalyst preparation

The monodispersed SiO_2 was prepared by the Stöber method [19]. In a typical synthesis, the mixture solution of 21 mL tetraethylorthosilicate (TEOS, 99.5%, SCRC) and 50 mL anhydrous ethanol (99.7%, SCRC) was added slowly into the mixed solution of 76 mL $NH_3 \cdot H_2O$ (26 vol.%, SCRC) and 200 mL anhydrous ethanol. Then, this synthesis solution was aged for 4 h and separated centrifugally at 7000 r.p.m. Finally, the collected product was washed with de-ionized water and dried at 70 °C for 12 h. Before being used, the SiO_2 was calcined in static air at

* Corresponding author. Tel.: +86 21 6087 7221; fax: +86 21 6087 7231.
E-mail address: dsmao@sit.edu.cn (D. Mao).

0378-3820/$ – see front matter © 2012 Elsevier B.V. All rights reserved.
http://dx.doi.org/10.1016/j.fuproc.2012.08.020

different temperatures (90 °C, 350 °C, and 550 °C) for 4 h, which were denoted as SiO_2(90), SiO_2(350), and SiO_2(550), respectively.

$RhCl_3$ hydrate (Rh ~36 wt.%, Fluka), $Mn(NO_3)_2 \cdot 6H_2O$ (99.99%, SCRC), Li_2CO_3 (99.5%, SCRC), and SiO_2 mentioned above were used in catalyst preparations. Catalysts were prepared by co-impregnation to incipient wetness of the prepared silica (1.0 g) with an aqueous solution of $RhCl_3$ hydrate and aqueous solutions of precursors of the promoters, followed by drying at 90 °C for 4 h, and then at 120 °C overnight before being calcined in air at 350 °C for 4 h. For all catalysts, Rh loading was 1.5 wt.% and the weight ratio of Rh:Mn:Li = 1.5:1.5:0.07. The obtained catalysts were denoted as RML/SiO_2(90), RML/SiO_2(350), and RML/SiO_2(550), respectively.

2.2. Reaction

CO hydrogenation was performed in a fixed-bed micro-reactor with length ~350 mm and internal diameter ~5 mm. The catalyst (0.3 g) diluted with inert α-alumina (1.2 g) was loaded between quartz wool and axially centered in the reactor tube, with the temperature monitored by a thermocouple close to the catalyst bed. Prior to reaction, the catalyst was heated to 400 °C (heating rate ~3 °C min^{-1}) and reduced with H_2/N_2 (10% *v/v*, total flow rate = 50 mL min^{-1}) for 2 h at atmospheric pressure. The catalyst was then cooled down to 290 °C and the reaction started at a space velocity (SV) of 10,000 mL g^{-1} h^{-1} and pressure of 3 MPa. The feed gas contained 60 vol.%H_2, 30 vol.% CO and 10 vol.%N_2. All post-reactor lines and valves were heated to 150 °C to prevent product condensation [20]. The products were analyzed by an on-line GC (Agilent 6820) using a HP-PLOT/Q column (30 m, 0.32 mm ID) with an FID (flame ionization detector) and a TDX-01 column with a TCD (thermal conductivity detector). The conversion of CO was calculated based on the fraction of CO that formed carbon-containing products according to: %Conversion = $(\sum n_i M_i / M_{CO}) \cdot 100$, where n_i is the number of carbon atoms in product i; M_i is the percentage of product i detected, and M_{CO} is the percentage of CO in the feed. The selectivity of a certain product was calculated based on carbon efficiency using the formula $n_i C_i / \sum n_i C_i$, where n_i and C_i are the carbon number and molar concentration of the *i*th product, respectively.

2.3. Catalyst characterization

The BET surface areas of samples were obtained using N_2 adsorption at −196 °C on a Micromeritics ASAP 2020 M + C apparatus. Prior to N_2 adsorption, the samples were degassed under a vacuum of 10^{-1} Pa for 10 h at 200 °C.

CO adsorption was studied using a Nicolet 6700 FTIR spectrometer equipped with a DRIFT (diffuse reflectance infrared Fourier transform) cell with CaF_2 windows. The sample in the cell was pretreated in H_2/N_2 (10% *v/v*) at 400 °C for 2 h, and then the temperature was dropped to room temperature (RT). After the cell was outgassed in vacuum to $<10^{-3}$ Pa, the background was scanned. After introducing CO into the IR cell ($p_{co} = 8.0 \times 10^3$ Pa), the IR spectrum of CO adsorbed on the catalyst was recorded. The concentration of CO was higher than 99.97%, and it was pretreated by dehydration and deoxygenization before being used. The spectral resolution was 4 cm^{-1} and the scan times were 64.

H_2 temperature-programmed desorption (H_2-TPD) as well as H_2 temperature-programmed reduction (H_2-TPR) and CO temperature-programmed desorption (CO-TPD) were carried out in a quartz microreactor. For H_2 or CO TPD measurements, the catalyst (0.1 g) was reduced in-situ for 2 h at 400 °C in H_2/N_2 (10% *v/v*), and then was held at 400 °C for another 30 min before being cooled down to RT in He flow. The next step was H_2 or CO adsorption at RT for 0.5 h, and then the gas was swept again with He for 3 h. Subsequently, the sample was heated in a flowing He stream (50 mL min^{-1}) up to ~500 °C at a rate of 10 °C min^{-1}, while the desorbed species was detected with a TCD detector for the H_2-TPD and a quadruple mass spectrometer (QMS, Balzers OmniStar 200) as the detector for CO-TPD process, respectively. The amount of hydrogen adsorption of various catalysts was calculated on the basis of their H_2-TPD profiles. For TPR measurements, 0.05 g of the sample was first pretreated at 350 °C in O_2/N_2 (20% *v/v*) for 1 h prior to a TPR measurement. During the TPR experiment, H_2/N_2 (10% *v/v*) was used at 50 mL min^{-1} and the temperature was ramped from RT to 650 °C at 10 °C min^{-1} while the effluent gas was analyzed with a TCD detector.

The TPSR experiment was carried out as follows: after the catalyst was reduced at 400 °C in H_2/N_2 (10% *v/v*) for 2 h, it was cooled down to RT and CO was introduced for adsorption for 0.5 h; afterward, the H_2/N_2 mixture was swept again, and the temperature was increased at the rate of 10 °C min^{-1} with the QMS as the detector to monitor the signals of CO (m/z = 28), CO_2 (m/z = 44), and CH_4 (m/z = 15).

3. Results and discussion

3.1. Catalytic activities

Table 1 shows the catalytic performances of the Rh – Mn – Li/SiO_2 catalysts for CO hydrogenation. It can be seen that the catalytic activities of the Rh – Mn – Li/SiO_2 catalysts dropped with the increase of the calcination temperature of SiO_2. However, the turnover frequency (TOF) of CO conversion, which was calculated on the base of the amount of chemisorbed H_2 determined by H_2-TPD (see next), over RML/SiO_2(350) was the highest. With respect to selectivity, the highest C_2 oxygenates selectivity followed with the lowest C_2^+ hydrocarbons selectivity was obtained on RML/SiO_2(350) catalyst. Compared with the catalysts of RML/SiO_2(90) and RML/SiO_2(550), the undesirable by-products of CO_2, hydrocarbons, and methanol all appeared to be suppressed over the catalyst of RML/SiO_2(350), in which the space time yield (STY) of C_2 oxygenates (274.1 g kg^{-1} h^{-1}) was the highest.

Table 1
Performance for CO hydrogenation on different Rh – Mn – Li/SiO_2 catalysts.

Catalyst	CO conv. (C%)	TOF[a] (s^{-1})	Selectivity of products[b] (C%)						STY(C_2 Oxy) (g kg^{-1} h^{-1})
			CO_2	CH_4	MeOH	C_2 Oxy[c]	C_2^+ HC[d]	Other Oxy[e]	
RML/SiO_2(90)	19.2	0.140	4.7	12.6	8.4	28.8	43.8	1.7	155.4
RML/SiO_2(350)	14.6	0.181	1.8	9.1	2.6	55.4	28.8	2.3	274.1
RML/SiO_2(550)	9.9	0.099	6.8	8.7	3.7	45.7	32.3	2.8	122.6

Reaction conditions: 290 °C, 3 MPa, SV = 10,000 mL g^{-1} h^{-1}, V(H_2)/V(CO) = 2, data taken after 15 h when steady state reached. Experimental error: ±5%.
[a] TOF based on CO conversion and H_2 chemisorption.
[b] Based on carbon efficiency, carbon selectivity = $n_i C_i / \sum n_i C_i$.
[c] C_2 Oxy denotes oxygenates containing two carbon atoms.
[d] C_2^+ HC denotes hydrocarbons containing two and more carbon atoms.
[e] Other Oxy denotes oxygenates containing more than two carbon atoms.

3.2. Characterization of SiO_2 support

N_2 adsorption-desorption was carried out to characterize the textural properties of the SiO_2 supports. It can be seen from Table 2 that SiO_2(90) had a large specific surface area of 268.3 $m^2\ g^{-1}$ and small average pore diameter of 2.2 nm. Compared with the support of SiO_2(90), the supports of SiO_2(350) and SiO_2(550) kept a smaller specific surface area (~11 $m^2\ g^{-1}$) and bigger average pore diameter (6–8 nm). It can be inferred that there are large amounts of surface functional groups of Si–OH on SiO_2(90), resulting in a large specific surface area. After the sample was calcined at 350 or 550 °C, the surface Si–OH groups on SiO_2 condensed significantly, leading to the similar structure of small specific surface area and big average pore diameter.

The IR spectra of the SiO_2 in N_2 atmosphere at 300 °C are presented in Fig. 1. According to the previous studies [14,21], the region in the range 3500–2750 cm^{-1} with a maximum at 3400 cm^{-1}, originates from the absorption of H_2O and –OH interacted with hydrogen bond; and the band at 950 cm^{-1}, arises from the absorption of Si–OH. As shown in Fig. 1, with increasing the calcination temperature, the intensities of the peaks at 3400 and 950 cm^{-1} become weaker, and the peak at 950 cm^{-1} disappeared completely when the calcination temperature was increased to 550 °C.

The previous studies [12,22–25] proved that the surface hydroxyl groups on SiO_2 has a strong interaction with the metal particles (e.g., Rh, Mn), and further affects the metal dispersion and interaction. Based on the different catalytic performances of Rh–Mn–Li/SiO_2 catalysts, it is suggested that the change of concentration of silica surface hydroxyls caused by different calcination temperature might be the direct factor for the different catalytic performances.

3.3. Characterization of Rh–Mn–Li/SiO_2 catalysts

3.3.1. Structural and textural properties

The textural properties of the supported catalysts are shown in Table 3. It can be seen that the supported catalysts all kept a similar specific surface area (12–16 $m^2\ g^{-1}$) and average pore diameter (6–8 nm). This result is consistent with the above conclusion that the group of Si-OH on SiO_2 surface condensed after the samples calcined at the higher temperature, resulting in the similar structure of small specific surface area and big average pore diameter. This result further confirmed that the different catalytic performances of the catalysts were not caused by their textural properties.

In the XRD patterns of the prepared catalysts (not shown), no discernable peaks related to any crystalline phase can be observed, indicating that the metal particles are highly dispersed.

The IR spectra of the catalysts at 300 °C and in N_2 atmosphere are presented in Fig. 2. It can be found that the IR profiles of the catalysts did not change obviously compared with the corresponding supports, but the intensity of the hydroxyl groups on SiO_2 decreased after supporting metal components, suggesting that the metal components were fixed by the hydroxyl-metal interaction.

3.3.2. H_2-TPD

The H_2-TPD profiles of various catalyst samples after reduction at 400 °C are shown in Fig. 3. The amount of hydrogen adsorption of various catalysts calculated on the basis of their H_2-TPD profiles is summarized in Table 4. It can be seen that there was only one peak

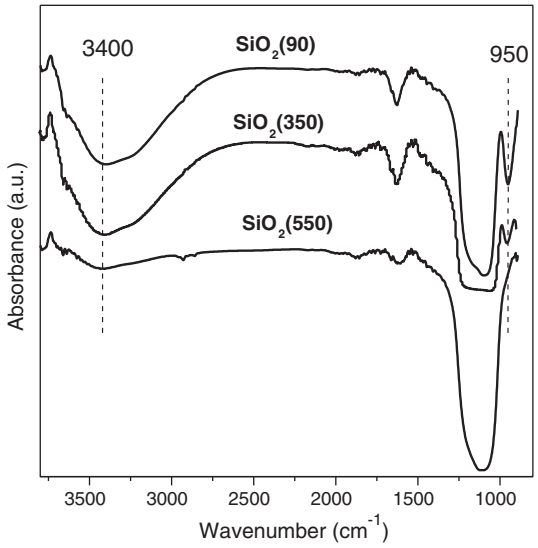

Fig. 1. IR spectra of the SiO_2 supports.

of H_2 desorption in the TPD profiles for all the catalysts, while the peak area decreased with the increase of the calcination temperature. When the calcination temperature of SiO_2 increased from 90 °C to 550 °C, the amount of chemisorbed H_2 decreased from 51.2 μmol g^{-1} for RML/SiO_2(90) to 29.8 μmol g^{-1} for RML/SiO_2(550). Considering that the surface hydroxyls of SiO_2 can be removed by calcination, it is suggested that the lower concentration of surface hydroxyls on silica caused by higher calcination temperature gave rise to a weaker interaction between the support and the added components during impregnation, leading to a lower Rh dispersion or yielding larger Rh particles [16,26]. It is obvious that lower Rh dispersion obtained on the SiO_2 calcined at higher temperature resulted in the lower Rh efficiency, which is consistent with the activity of the catalysts.

3.3.3. H_2-TPR

Fig. 4 shows the H_2-TPR profiles for all the catalysts. There were three peaks of H_2 consumption in the TPR profiles of the catalysts. According to the research of Ding and co-workers [27,28], the high temperature peak centered at 200 °C is ascribed to the reduction of MnO_2; the major peak at ~130 °C and the shoulder at ~150 °C are ascribed to the reduction of Rh_2O_3 not intimately contacting with Mn species (denoted as Rh(I)) and of Rh_2O_3 intimately contacting with Mn species (denoted as Rh(II)), respectively. As shown in Fig. 4, with increasing the calcination temperature, the reduction peak of MnO_2 moved to the lower temperature in company with the increase of its intensity, while the ratio of Rh(II) versus Rh(I) was increased.

Many studies have showed that the addition of Mn in the Rh-based catalyst would increase the reduction temperature of Rh oxides, and decrease the reduction temperature of Mn oxides [17,28,29]. Thus the width of temperature region between Rh and Mn oxides reduction peaks can be a judge for the strength of Rh-Mn interaction: the small width of temperature region between Rh and Mn oxides reduction peaks indicates a strong Rh-Mn interaction. Combined with the hydroxyls information of the supports observed by FT-IR (Fig. 1), it is proposed that less hydroxyl groups left on the SiO_2 calcined at higher

Table 2
Specific surface areas (S_{BET}), pore volume (V_p) and pore diameter (D_p) of the supports.

Sample	S_{BET} ($m^2\ g^{-1}$)	V_p ($cm^3\ g^{-1}$)	D_p (nm)
SiO_2(90)	268.3	0.053	2.2
SiO_2(350)	11.6	0.021	7.9
SiO_2(550)	10.9	0.027	9.3

Table 3
Specific surface areas (S_{BET}), pore volume (V_p) and pore diameter (D_p) of the catalysts.

Sample	S_{BET} ($m^2\ g^{-1}$)	V_p ($cm^3\ g^{-1}$)	D_p (nm)
RML/SiO_2(90)	16.2	0.029	7.3
RML/SiO_2(350)	13.4	0.021	6.7
RML/SiO_2(550)	12.3	0.026	7.9

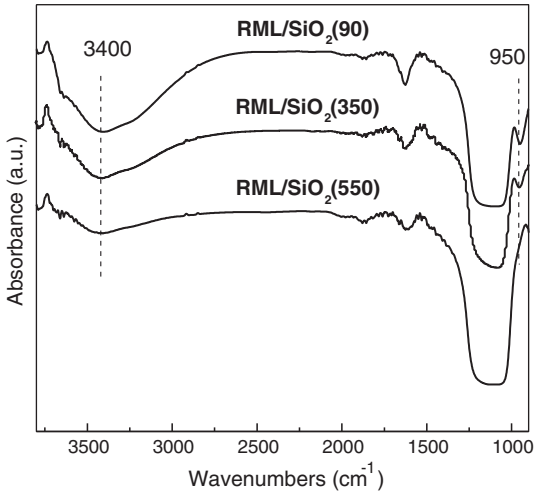

Fig. 2. IR spectra of the catalysts.

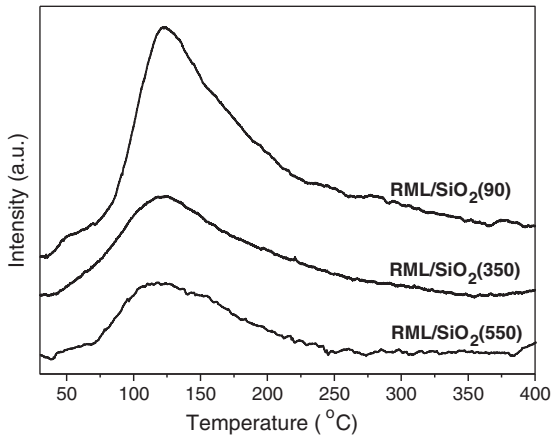

Fig. 3. H_2-TPD profiles of the catalysts.

temperature, which decreased the metal dispersion and enhanced the Rh-Mn interaction.

3.3.4. FT-IR

The IR spectra of the *in situ* reduced catalysts interacting with 80 mbar CO in vacuum at 30 °C for 30 min are shown in Fig. 5. The IR spectrum was mainly composed by a doublet at 2104 and 2030 cm^{-1} and a band at around 2067 cm^{-1}. The doublet can be assigned to the symmetric and asymmetric carbonyl stretching of the gem-dicarbonyl $Rh^+(CO)_2$ [CO(gdc)] and the 2067 cm^{-1} band can be attributed to the linear adsorbed CO [CO(l)] [30]. Meanwhile, the band at around 1840 cm^{-1} is assigned to the bridge bonded CO [CO(b)] [31]. It is widely accepted that the dicarbonyl species can only be formed on the Rh^+ sites which may be highly dispersed and linear CO be on the Rh^0 sites [32,33]. It can be seen that the intensity of adsorbed CO and the ratio of germinal versus linear CO (Rh^+/Rh^0) on the catalysts declined with the increase in calcination temperature of the SiO_2, suggesting that high Rh dispersion was achieved by the assisting of hydroxyl-metal interaction, which is in line with the

Table 4
H_2 chemisorption data for the catalysts.

Catalyst	RML/SiO_2(90)	RML/SiO_2(350)	RML/SiO_2(550)
H_{2ads} (μmol g^{-1})	51.2	37.1	29.8

Experimental error: ±5%.

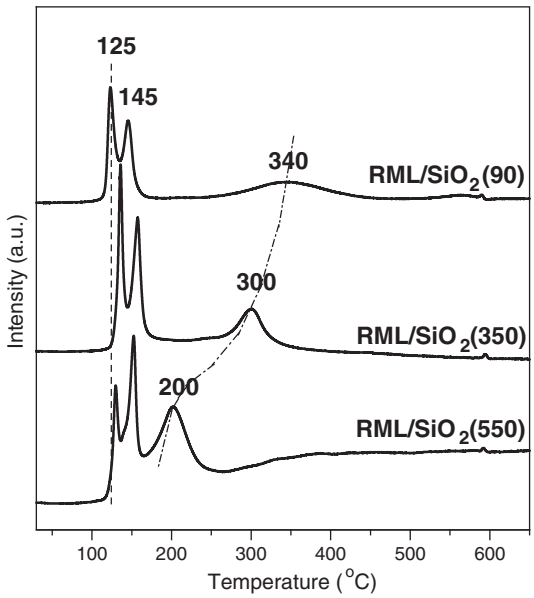

Fig. 4. H_2-TPR profiles of the catalysts.

result of H_2-TPD. Moreover, this situation is also similar to the reported view that the hydrated ions of $Co(H_2O)_6^{2+}$ may be related to the silica surface hydroxyls by the effect of hydrogen bonds, and these hydrogen bonds block the aggregation of the cobalt species, resulting in a higher metal dispersion [34].

As discussed above, it can be concluded that the lower concentration of silica surface hydroxyls caused by higher calcination temperature weakened the hydroxyl-metal interaction, which decreased the Rh dispersion and CO adsorption, and resulted in lower CO inversion.

3.3.5. CO-TPD and TPSR

The desorption profiles of CO (m/z = 28) in Fig. 6 show that the similar associative desorption of CO take place on various catalysts, suggesting comparable strength of interaction of CO with respective catalyst surfaces. According to the research reported previously [35], the thermal stability of various types of CO adsorbed on Rh of the highly dispersed Rh/SiO_2-based catalyst is in the following order: CO(b) > CO(gdc) > CO(l). So, the peak at around 120 °C should correspond to CO(l) species, and the peak at 160 °C may be due to CO(gdc)

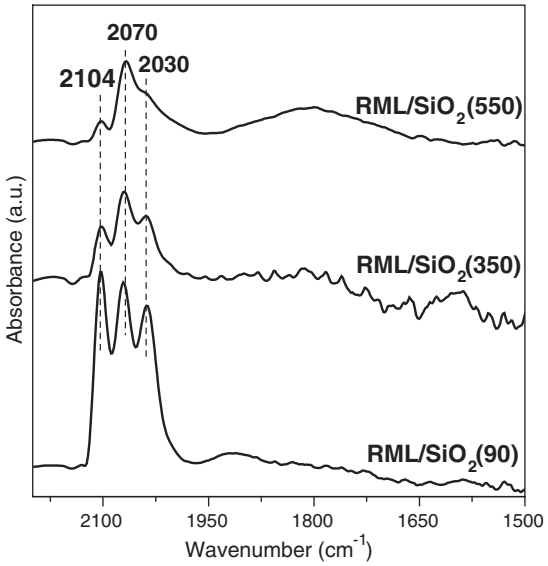

Fig. 5. FT-IR spectra of CO adsorbed on different catalysts.

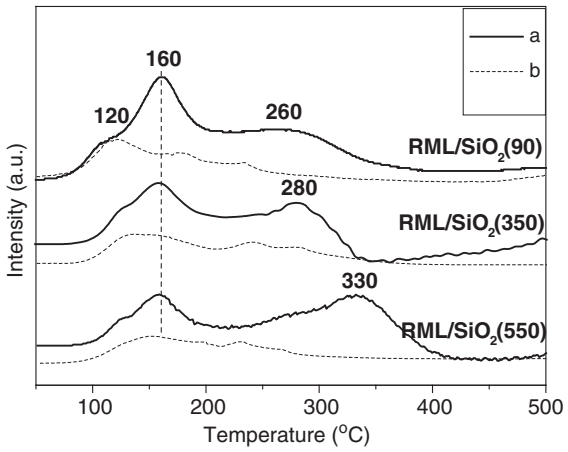

Fig. 6. The profiles of CO desorption: (a) CO desorbed during CO-TPD process; (b) CO desorbed during TPSR process.

species, while the peak exceeded 230 °C may be assigned to the desorption of bridge-bonded CO [CO(b)] species or the other forms [36]. It is obvious that the desorption amount of CO(l) and CO(gdc) is consistent with the intensity of adsorbed CO discussed in section 3.3.4.

Meanwhile, the profiles of CO desorbed during TPSR are compared with the CO desorbed during CO-TPD. It can be seen that only a broad peak between 100 °C and 250 °C existed in the profiles of TPSR, and the peak above 250 °C could no longer be detected in the TPSR process. Considering that the peak of CH_4 also appeared after 200 °C, it is obvious that CH_4 is formed at the expense of the strongly adsorbed CO species. Of course, the amount of CO(l) and CO(gdc) also decreased during TPSR process, and only a broad peak at around 150 °C was left. It is guessed that H_2 spillover might occur on the catalysts at low temperature, and the adsorbed CO is activated and transfers into other adsorption forms [9].

Since the hydrogenation of dissociated CO into CH_4 is very fast on the Rh-based catalyst, the methane formation in TPSR can be used as a tool for measuring the CO dissociation over such catalysts [17]. Fig. 7 shows the profiles of CH_4 production on the catalysts. It can be seen

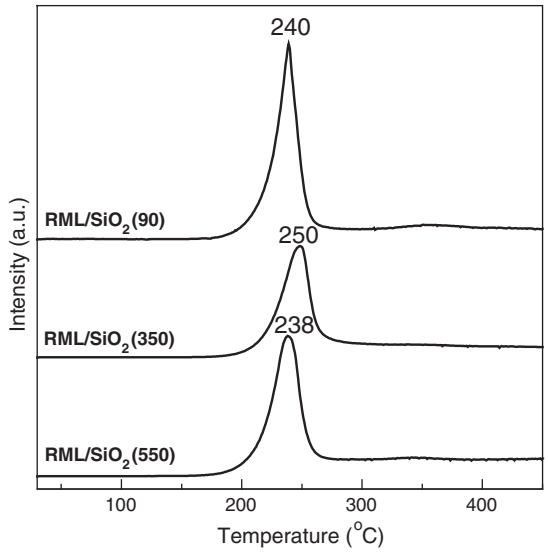

Fig. 7. CH_4 formation on the catalysts during TPSR process.

that on the profiles of RML/SiO_2(90) and RML/SiO_2(550) catalysts, the peaks of CH_4 formation were centered at around 240 °C; however, the CH_4 peak shifted to 250 °C on RML/SiO_2(350) catalyst, suggesting that weaker hydrogenation ability was obtained on it. In addition, the amount of CH_4 produced by the catalysts were different, following the order as shown in Fig. 6: RML/SiO_2(90) > RML/SiO_2(550) > RML/SiO_2(350), that is to say, the hydrogenation ability decreased in the same order, which is consistent with the result of hydrocarbons selectivity of the catalysts.

It is usually considered that the formation of hydrocarbons from CH_x hydrogenation and the formation of C_2 oxygenates from CO insertion are the couple of competitive reaction, and the relative reaction rate between them determines the activity and selectivity forwards C_2 oxygenates [37]. In order to get a high yield of C_2 oxygenates, it need a catalyst which has the moderate CO dissociation and hydrogenation activity. Combined with the reactive performance, it is suggested that the moderate hydrogenation activity exhibited on RML/SiO_2(350) is conducive to the reaction of CO insertion, thus it obtained the highest selectivity forwards C_2 oxygenates.

Based on the above results, it can be concluded that when the calcination temperature is too low (90 °C), the Rh – Mn interaction is very weak and the promotion effect of Mn is hardly to show, which is not favorable for the formation of C_2 oxygenates; while the calcination temperature is too high (550 °C), the strong Rh – Mn interaction decreased the ability of CO adsorption and catalytic activity. However, a moderate interaction between Rh and Mn can be obtained on the SiO_2 calcined at 350 °C. This is not only conducive to exert the promoting effect of Mn promoter and gain the moderate hydrogenation ability, but also promotes the reaction of CO insertion, finally resulting in the best catalytic performance for the synthesis of C_2 oxygenates. The effect of drying time on the catalytic performance of Rh – Mn – Li/SiO_2 studied by Chen et al. [38] also emphasized that the good catalytic performance just can be gained when the Rh-Mn interaction at the appropriate intensity, which is consistent with our conclusion.

4. Conclusions

The catalysts of Rh – Mn – Li/SiO_2 were prepared by co-impregnation using the monodispersed SiO_2 calcined at different temperatures as the supports, then followed by calcination and reduction before being used for CO hydrogenation in a fixed-bed reactor at 290 °C and 3 MPa. The results showed that changing of the calcination temperature could effectively regulate the amount of surface Si – OH groups on SiO_2, and further changed the metal dispersion and Rh – Mn interaction. The results of H_2-TPD as well as FT-IR and CO-TPD proved that the increasing amount of Si – OH groups was favorable for the Rh dispersion and CO adsorption, thus enhanced the activity of the catalyst. Combing the results of H_2-TPR and TPSR, it is concluded that an appropriate amount of Si – OH groups can gain a moderate interaction between Rh and Mn. This interaction is conducive to achieve the right hydrogenation ability, which is favorable for the reaction of CO insertion, and ultimately increases the selectivity of C_2 oxygenates.

Acknowledgment

The authors acknowledge financial supports from the Science and Technology Commission of Shanghai Municipality (08520513600), Leading Academic Discipline Project of Shanghai Education Committee (J51503) and Shanghai Institute of Technology (KJ2011-02).

References

[1] J.R. Rostrup-Nielsen, Making fuels from biomass, Science 308 (2005) 1421–1422.
[2] V. Subramani, S.K. Gangwal, A review of recent literature to search for an efficient catalytic process for the conversion of syngas to ethanol, Energy & Fuels 22 (2008) 814–839.

[3] J.J. Spivey, A. Egbebi, Heterogeneous catalytic synthesis of ethanol from biomass-derived syngas, Chemical Society Reviews 36 (2007) 1514–1528.
[4] D.H. Mei, R. Rousseau, S.M. Kathmann, V.A. Glezakou, M.H. Engelhard, W.L. Jiang, Ethanol synthesis from syngas over Rh-based/SiO_2 catalysts: a combined experimental and theoretical modeling study, Journal of Catalysis 271 (2010) 325–342.
[5] G.C. Chen, C.Y. Guo, X.H. Zhang, Z.J. Huang, G.Q. Yuan, Direct conversion of syngas to ethanol over Rh/Mn-supported on modified SBA-15 molecular sieves: effect of supports, Fuel Processing Technology 92 (2011) 456–461.
[6] H.M. Yin, Y.J. Ding, H.Y. Luo, L. Yan, T. Wang, L.W. Lin, The performance of C_2 oxygenates synthesis from syngas over Rh – Mn – Li – Fe/SiO_2 catalysts with various Rh loadings, Energy & Fuels 17 (2003) 1401–1406.
[7] X.M. Yang, Y. Wei, Y.L. Su, L.P. Zhou, Characterization of fused Fe – Cu based catalyst for higher alcohols synthesis and DRIFTS investigation of TPSR, Fuel Processing Technology 91 (2010) 1168–1173.
[8] H.Y. Luo, P.Z. Lin, S.B. Xie, H.W. Zhou, C.H. Xu, S.Y. Huang, The role of Mn and Li promoters in supported rhodium catalysts in the formation of acetic acid and acetaldehyde, Journal of Molecular Catalysis A: 122 (1997) 115–123.
[9] Y. Wang, Z. Song, D. Ma, H.Y. Luo, D.B. Liang, X.H. Bao, Characterization of Rh-based catalysts with EPR, TPR, IR and XPS, Journal of Molecular Catalysis A: 149 (1999) 51–61.
[10] J.R. Katzer, A.W. Sleight, P. Gajardo, J.B. Michel, E.F. Gleason, S. McMillan, The role of the support in CO hydrogenation selectivity of supported rhodium, Faraday Discussions of the Chemical Society 72 (1981) 121–133.
[11] S. Ho, Y. Su, Effects of ethanol impregnation on the properties of silica-supported cobalt catalysts, Journal of Catalysis 168 (1997) 51–59.
[12] D.H. Jiang, Y.J. Ding, Z.D. Pan, W.M. Chen, H.Y. Luo, CO hydrogenation to C_2-oxygenates over Rh – Mn – Li/SiO_2 catalyst: effects of support pretreatment with $nC_1 - C_5$ alcohols, Catalysis Letters 121 (2008) 241–246.
[13] F. Solymosi, I. Tombacz, M. Kocsis, Hydrogenation of CO on supported Rh catalysts, Journal of Catalysis 75 (1982) 78–93.
[14] P. Basu, D. Panayotov, J.T. Yates Jr., Rhodium-carbon monoxide surface chemistry: the involvement of surface hydroxyl groups on $A1_2O_3$ and SiO_2 supports, Journal of the American Chemical Society 110 (1988) 2074–2081.
[15] J. Yu, D.S. Mao, G.Z. Lu, Q.S. Guo, L.P. Han, Enhanced C_2 oxygenate synthesis by CO hydrogenation over Rh-based catalyst supported on a novel SiO_2, Catalysis Communications 24 (2012) 25–29.
[16] R. Burch, M.J. Hayes, The preparation and characterisation of Fe-promoted Al_2O_3-supported Rh catalysts for the selective production of ethanol from syngas, Journal of Catalysis 165 (1997) 249–263.
[17] M. Ojeda, M.L. Granados, S. Rojas, P. Terreros, F.J. García-García, J.L.G. Fierro, Manganese-promoted Rh/Al_2O_3 for C_2-oxygenates synthesis from syngas: effect of manganese loading, Applied Catalysis A: General 261 (2004) 47–55.
[18] A. Boffa, C. Lin, A.T. Bell, G.A. Somorjai, Promotion of CO and CO_2 hydrogenation over Rh by metal oxides: the influence of oxide Lewis acidity and reducibility, Journal of Catalysis 149 (1994) 149–158.
[19] M. Szekeres, O. Kamalin, P.G. Grobet, R.A. Schoonheydt, K. Wostyn, K. Clays, Two-dimensional ordering of Stöber silica particles at the air/water interface, Colloids and Surfaces A: Physicochemical and Engineering Aspects 227 (2003) 77–83.
[20] D.S. Mao, Q.S. Guo, J. Yu, L.P. Han, G.Z. Lu, Effect of cerium addition on the catalytic performance of Cu – Fe/SiO_2 for the synthesis of lower alcohols from syngas, Acta Physico-Chimica Sinica 27 (2011) 2639–2645.
[21] J.B. Peri, Infrared study of OH and NH_2 groups on the surface of a dry silica aerogel, Journal of Physical Chemistry 70 (1966) 2937–2945.
[22] W.M. Chen, Y.J. Ding, D.H. Jiang, Z.D. Pan, H.Y. Luo, An effective method of controlling metal particle size on impregnated Rh – Mn – Li/SiO_2 catalyst, Catalysis Letters 104 (2005) 177–180.
[23] H.T. Ma, Y. Wang, X.H. Bao, Study on the surface location of reactive metals of Rh – Mn/SiO_2 catalyst in ethanol synthesis from syngas, Acta Scientiarum Naturalium Universitatis Pekinensis 37 (2001) 210–214.
[24] F. Solymosi, M. Pasztor, An infrared study of the influence of carbon monoxide chemisorption on the topology of supported rhodium, Journal of Physical Chemistry 89 (1985) 4789–4793.
[25] F. Solymosi, M. Pasztor, Infrared study of the effect of hydrogen on carbon monoxide-induced structural changes in supported rhodium, Journal of Physical Chemistry 90 (1986) 5312–5317.
[26] W.M. Chen, Y.J. Ding, X.G. Song, T. Wang, H.Y. Luo, Promotion effect of support calcination on ethanol production from CO hydrogenation over Rh/Fe/Al_2O_3 catalysts, Applied Catalysis A: General 407 (2011) 231–237.
[27] H.M. Yin, Y.J. Ding, H.Y. Luo, H.J. Zhu, D.P. He, J.M. Xiong, Influence of iron promoter on catalytic properties of Rh – Mn – Li/SiO_2 for CO hydrogenation, Applied Catalysis A: General 243 (2003) 155–164.
[28] D.H. Jiang, Y.J. Ding, Z.D. Pan, X.M. Li, G.P. Jiao, J.W. Li, Roles of chlorine in the CO hydrogenation to C_2-oxygenates over Rh – Mn – Li/SiO_2 catalysts, Applied Catalysis A: General 331 (2007) 70–77.
[29] M.A. Haider, M.R. Gogate, R.J. Davis, Fe-promotion of supported Rh catalysts for direct conversion of syngas to ethanol, Journal of Catalysis 261 (2009) 9–16.
[30] S.D. Worley, G.A. Mattson, R. Caudlll, An infrared study of the hydrogenation of carbon monoxide on supported rhodium catalysts, Journal of Physical Chemistry 87 (1983) 1671–1673.
[31] A.C. Yang, C.W. Garland, Infrared studies of carbon monoxide chemisorbed on rhodium, Journal of Physical Chemistry 61 (1957) 1504–1512.
[32] R.R. Cavanagh, J.T. Yates Jr., Site distribution studies of Rh supported on Al_2O_3 — an infrared study of chemisorbed CO, Journal of Chemical Physics 74 (1981) 4150–4155.
[33] C.A. Rice, S.D. Worley, C.W. Curtis, J.A. Guin, A.R. Tarrer, The oxidation state of dispersed Rh on Al_2O_3, Journal of Chemical Physics 74 (1981) 6487–6497.
[34] J.G. Chen, H.W. Xiang, Y.H. Sun, Influence of silica sources on performance of Co/SiO_2 catalysts for F-T synthesis, Chinese Journal of Catalysis 21 (2000) 169–171.
[35] R. Ugo, The contribution of organometallic chemistry and homogeneous catalysis to the understanding of surface reactions, Catalysis Reviews 11 (1975) 255–297.
[36] Y. Wang, H.Y. Luo, D.B. Liang, X.H. Bao, Different mechanisms for the formation of acetaldehyde and ethanol on the Rh-based catalysts, Journal of Catalysis 196 (2000) 46–55.
[37] Y.M. Choi, P. Liu, Mechanism of ethanol synthesis from syngas on Rh(111), Journal of the American Chemical Society 131 (2009) 13054–13061.
[38] W.M. Chen, Y.J. Ding, H.Y. Luo, L. Yan, T. Wang, Z.D. Pan, Influence of preparation method and conditions on performance of Rh – Mn – Li – Ti/SiO_2 catalyst for CO hydrogenation to C_2-oxygenates, Chinese Journal of Applied Chemistry 22 (2005) 470–474.